

Supporting Information

Realization of switching between TADF and HLCT emissions through modulation of the intramolecular charge transfer character

Jiaqi Li, Mingfan Zhang, Tingyu Li, Dongxue Guo, Tian Tian, and Houyu Zhang*

State key laboratory of supramolecular structure and materials,

Institute of theoretical chemistry, College of Chemistry, Jilin university,

Changchun 130012, P.R. China

*Email: houyuzhang@jlu.edu.cn

Contents

Table S1. Calculated HOMO energies of molecule **TPA-BZP** with different DFT functionals.

Table S2. Calculated absorption and emission wavelengths of **TPA-BZP** with different functionals.

Table S3. Calculated $\Delta E_{T_2-T_1}$ of the TPA-based D-A type molecules and different acceptor units.

Table S4. NTO distributions and main transition excitations of acceptor fragments.

Table S5. Calculated HOMO-LUMO overlap integral and charge transfer amount in S_0 state.

Table S6. Calculated HOMO and LUMO levels of the donor and acceptor segments.

Table S7. Calculated absorption wavelengths and energies, oscillator strengths, and dominant orbital excitations from TD-DFT calculation.

Table S8. Calculated the related orbital distributions and vertical excitation energies of LE states.

Table S9. Calculated vertical excitation energies and gaps of the investigated molecules.

Table S10. Calculated adiabatic excitation energies and gaps of the investigated molecules.

Table S11. Calculated $\Delta E_{T_2-T_1}$ and NAC constants between T_1 and T_2 states by ORCA package.

Table S12. Calculated parameters for the state hybridization of LE and CT states.

Table S13. Calculated dihedral angles for the investigated molecules in ground and excited states.

Table S14. Calculated parameters for the state hybridization of LE and CT states for the investigated D-A-D type molecules.

Table S15. Calculated vertical excitation energies of singlet and triplet states, energy gaps, SOC and NAC constants, k_{RISC} , k_p and k_f of the investigated molecules.

Figure S1. The TDM maps, the overlaps and distributions of electron-hole wavefunctions of the **BF**-based molecules.

Figure S2. NTO analysis for excited states and related energy diagrams of the state hybridization between LE and CT states for both singlet and triplet subspaces.

Figure S3. Calculated emission energies and oscillator strengths in S_1 states of the **POZ**-based molecules as function of the twisted angles.

Figure S4. Chemical structures of the investigated D-A-D type molecules.

Figure S5. NTO analysis for the related excited states and energy diagrams of the state hybridization between LE and CT states for D-A-D type HLCT molecules.

Figure S6. NTO analysis for the related excited states and energy diagrams of the state hybridization between LE and CT states for D-A-D type TADF molecules.

Table S1. Calculated HOMO energies of molecule **TPA-BZP** with different DFT functionals with a fixed percentage of nonlocal Hartree-Fock exchange (HF_{exc}).

	B3LYP	PBE0	BMK	CAM-B3LYP	Exptl. ^a
HF_{exc}	20%	25%	42%	19% at SR and 65% at LR	
HOMO (eV)	-4.95	-5.18	-5.61	-6.19	-5.22

^aExptl: from ref. 35.

Table S2. Calculated absorption wavelength (λ_{abs}) and emission wavelength (λ_{em}) of molecule **TPA-BZP** with different DFT functionals with a fixed percentage of nonlocal Hartree-Fock exchange (HF_{exc}).

	B3LYP	PBE0	BMK	CAM-B3LYP	Exptl. ^a
HF_{exc}	20%	25%	42%	19% at SR and 65% at LR	
λ_{abs} (nm)	544	508	433	398	436
λ_{em} (nm)	687	611	527	509	523

^aExptl: from ref. 35.

Table S3. Calculated $\Delta E_{T_2-T_1}$ of the TPA-based D-A type molecules and different acceptor units.

Mol.	$\Delta E_{T_2-T_1}$ (D-A)	$\Delta E_{T_2-T_1}$ (A)
TPA-AN	1.38 (1.31) ^a	1.58 (1.62) ^a
TPA-AC	1.15 (1.12) ^b	1.44
TPA-NZP	1.50 (1.60) ^c	1.79 (1.51) ^c
TPA-DPPZ	0.47 (0.90) ^d	0.40
TPA-BZP	1.00 (0.97) ^e	1.00

^{a, b, c, d, e}: Data in parentheses are respectively from ref. 46, 48, 50, 37, 35.

Table S4. NTO distributions and main transition excitations of T_1 and T_2 states for various acceptor fragments, estimated by TD-DFT at the BMK/6-31G (d, p) level.

	State	Excitation	NTOs	
			Hole	Electron
AN	T_1	$H \rightarrow L$ (95.8%)		
	T_2	$H-2 \rightarrow L$ (51.8%) $H \rightarrow L+2$ (40.8%)		
AC	T_1	$H \rightarrow L$ (94.7%)		
	T_2	$H-3 \rightarrow L$ (61.9%) $H \rightarrow L+2$ (31.8%)		
NZ	T_1	$H \rightarrow L$ (99.7%)		
	T_2	$H-1 \rightarrow L$ (96.5%)		
DPPZ	T_1	$H \rightarrow L$ (56.1%) $H-2 \rightarrow L$ (25.2%)		
	T_2	$H-3 \rightarrow L$ (89.8%)		
	T_3	$H-1 \rightarrow L$ (90.4%)		
	T_4	$H-2 \rightarrow L$ (31.5%) $H \rightarrow L+2$ (25.3%) $H-4 \rightarrow L$ (11.9%)		
BZ	T_1	$H \rightarrow L$ (94.9%)		
	T_2	$H-1 \rightarrow L$ (98.5%)		
BZP	T_1	$H \rightarrow L$ (81.9%)		
	T_2	$H-2 \rightarrow L$ (92.5%)		
BF	T_1	$H \rightarrow L$ (83.0%) $H \rightarrow L+1$ (5.7%)		
	T_2	$H-1 \rightarrow L$ (77.9%) $H-1 \rightarrow L+2$ (7.2%)		

Table S5. Calculated HOMO-LUMO overlap integral (β) and charge transfer amount (q) of the investigated molecules in S_0 state.

Mol.	TPA-BZP	TPA-BF	POZ-BZP	POZ-BF
$\beta(S_0)$	0.4167	0.3299	0.1234	0.1345
q	0.8125	0.8293	0.9162	0.9306

Table S6. Calculated HOMO and LUMO levels of the donor fragments **TPA** and **POZ**, and acceptor units **BZ** and **BF** at the PBE0/6-31G (d, p) level.

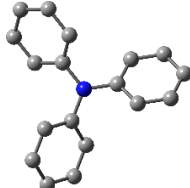
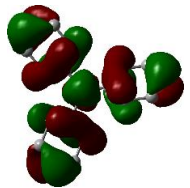
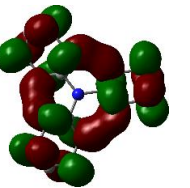
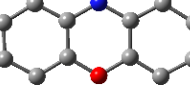
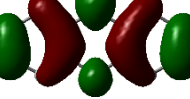
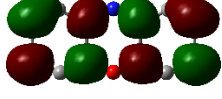
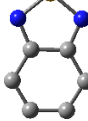
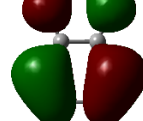
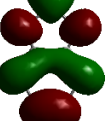
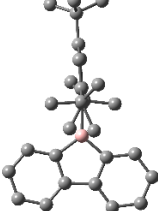
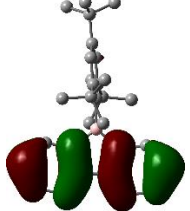
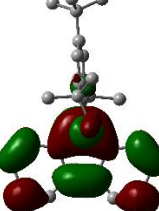
	Structure	HOMO	LUMO
TPA			-5.18 eV 
POZ			-4.92 eV 
BZ			-6.91 eV 
BF			-6.09 eV 

Table S7. Calculated absorption wavelengths (λ) and energies (ΔE), oscillator strengths (f), and dominant orbital excitations from TD-DFT calculation for the molecules.

Mol.	State	λ (nm)	ΔE (eV)	f	Excitation
TPA-BZP	S ₁	433	2.87	0.4849	H → L (93%)
	S ₂	332	3.73	0.0440	H-1 → L (91%)
	T ₁	624	1.99	0	H → L (46%); H-1 → L (43%)
	T ₂	414	2.99	0	H → L (30%); H → L +1 (15%)
TPA-BF	S ₁	398	3.12	0.1265	H → L (62%); H-1 → L (35%)
	S ₂	329	3.77	0.2157	H → L (26%); H-1 → L (44%)
	T ₁	502	2.47	0	H → L (33%); H-1 → L (49%)
	T ₂	391	3.17	0	H → L+1 (40%); H → L+4 (21%)
POZ-BZP	S ₁	587	2.11	0	H → L (98%)
	S ₂	338	3.67	0.2865	H-2 → L (98%)
	T ₁	591	2.10	0	H → L (97%)
	T ₂	542	2.29	0	H-2 → L (81%)
POZ-BF	S ₁	456	2.72	0.0015	H → L (97%)
	S ₂	359	3.46	0.0112	H-1 → L (91%)
	T ₁	471	2.63	0	H → L (44%); H-1 → L (43%)
	T ₂	451	2.75	0	H → L (50%); H-1 → L (33%)

Table S8. Calculated the related orbital distributions and vertical excitation energies of LE states.

	Hole	Particle	$E_{1_{LE}}$	$E_{3_{LE}}$
BF			3.41 eV	2.65 eV
BZP			3.43 eV	2.28 eV

Table S9. Calculated vertical excitation energies of singlet and triplet states, energy gaps between S_1 and related T_n states of the investigated molecules by BMK/6-31G (d, p) level (energy unit in eV).

Mol.	TPA-BZP (BZP)	TPA-BF (BF)	POZ-BZP	POZ-BF
E_{T_1}	1.99 (2.28) ^a	2.47 (2.66) ^a	2.10	2.63
E_{T_2}	2.99 (3.46) ^a	3.17 (3.64) ^a	2.29	2.75
E_{T_3}	3.47	3.46	3.17	3.10
E_{T_4}	3.48	3.51	3.47	3.57
E_{T_5}	3.54	3.65	3.71	3.59
E_{S_1}	2.87	3.12	2.11	2.72
E_{S_2}	3.73	3.77	3.67	3.47
$\Delta E_{T_2-T_1}$	1.00 (1.18) ^a	0.70 (0.98) ^a	0.19	0.12
$\Delta E_{S_1-T_1}$	0.88	0.65	0.01	0.09
$\Delta E_{S_1-T_2}$	-0.12	-0.05	-0.18	-0.03
Mol.	CZP-BZP	CZP-BF	DMAC-BZP	DMAC-BF
E_{T_1}	2.08	2.54	2.26	2.65
E_{T_2}	3.26	3.45	2.34	2.95
E_{T_3}	3.46	3.47	3.47	3.49
E_{T_4}	3.47	3.62	--	--
E_{T_5}	3.64	3.65	--	--
E_{S_1}	3.15	3.26	2.36	2.97
E_{S_2}	3.67	3.75	3.66	3.43
$\Delta E_{T_2-T_1}$	1.18	0.91	0.08	0.30
$\Delta E_{S_1-T_1}$	1.07	0.72	0.10	0.32
$\Delta E_{S_1-T_2}$	-0.11	-0.19	0.02	0.02

^a: Data in parentheses are parameters from acceptor units.

Table S10. Calculated adiabatic excitation energies of S_1 and T_1 states and their energy gaps at BMK/6-31G (d, p) level (energy unit in eV).

Mol.	TPA-BZP	TPA-BF	POZ-BZP	POZ-BF
$E_{T_1-S_0}$	1.80	1.93	1.77	1.92
$E_{S_1-S_0}$	2.62	2.62	1.77	2.28
ΔE_{ST}	0.82	0.69	0	0.36
Mol.	CZP-BZP	CZP-BF	DMAC-BZP	DMAC-BF
$E_{T_1-S_0}$	2.82	2.74	2.12	2.21
$E_{S_1-S_0}$	1.90	2.21	1.93	2.57
ΔE_{ST}	0.92	0.53	0.19	0.36

Table S11. Calculated $\Delta E_{T_2-T_1}$ and NAC constants between T_1 and T_2 states for the investigated molecules by ORCA package.

Mol.	POZ-BZP	POZ-BF	DMAC-BZP	DMAC-BF
$\Delta E_{T_2-T_1}$	0.19	0.12	0.08	0.30
NAC (bohr⁻¹)	3.43	2.11	3.30	2.68
Mol.	TPA-BZP	TPA-BF	CZP-BZP	CZP-BF
$\Delta E_{T_2-T_1}$	1.00	0.70	1.18	0.91
NAC (bohr⁻¹)	0.98	2.27	1.85	1.06

Table S12. Calculated parameters for the state hybridization of LE and CT states for the investigated molecules (energy unit in eV).

Mol.	$E_{1_{LE}}$	$E_{1_{CT}}$	ΔE	E_{S_1}	E_{S_2}	δE	J_S	η_s
CZP-BZP	3.43	3.39	0.02	3.15	3.67	0.52	0.26	6.50
CZP-BF	3.41	3.60	0.10	3.26	3.75	0.49	0.22	1.10
DMAC-BZP	3.43	2.59	0.42	2.36	3.66	1.30	0.50	0.60
DMAC-BF	3.41	2.99	0.21	2.97	3.43	0.46	0.10	0.24
Mol.	$E_{3_{LE}}$	$E_{3_{CT}}$	ΔE	E_{T_1}	E_{T_2}	δE	J_T	η_T
CZP-BZP	2.28	3.06	0.39	2.08	3.26	1.18	0.44	0.57
CZP-BF	2.65	3.34	0.34	2.54	3.45	0.91	0.30	0.44
DMAC-BZP	2.28	2.32	0.02	2.26	2.34	0.08	0.04	1.00
DMAC-BF	2.65(5)	2.94(3)	0.14(4)	2.65(3)	2.94(4)	0.29(1)	0.02(0)	0.06(9)

Table S13. Calculated dihedral angles (in degree) for the investigated molecules in the ground and excited states.

Mol.	S_0	S_1	T_1	$ S_0-S_1 $	$ S_0-T_1 $
CZP-BZP	36.4	14.1	14.6	22.3	21.8
CZP-BF	37.5	29.2	27.7	8.3	9.8
DMAC-BZP	86.0	89.9	61.0	3.9	25.0
DMAC-BF	89.5	85.5	59.8	4.0	29.2

Table S14. Calculated parameters for the state hybridization of LE and CT states for the investigated D-A-D type molecules (energy unit in eV).

Mol.	$E_{1_{LE}}$	$E_{1_{CT}}$	ΔE	E_{S_1}	E_{S_3}	δE	J_s	η_s
<i>o</i>-2CZP-BZ	3.43	3.71	0.14	3.20	3.94	0.74	0.34	1.22
<i>m</i>-2CZP-BZ	3.43	3.60	0.08	3.23	3.80	0.57	0.27	1.69
<i>p</i>-2CZP-BZ	3.43	3.36	0.04	3.00	3.79	0.79	0.39	4.87
<i>o</i>-2POZ-BZ	3.43	2.40	0.52	2.07	3.76	1.69	0.67	0.64
<i>m</i>-2POZ-BZ	3.43	2.40	0.52	2.07	3.82	1.75	0.71	0.68
<i>p</i>-2POZ-BZ	3.43	2.36	0.54	2.01	3.78	1.77	0.70	0.65
Mol.	$E_{3_{LE}}$	$E_{3_{CT}}$	ΔE	E_{T_1}	E_{T_n}	δE	J_t	η_t
<i>o</i>-2CZP-BZ	2.28	3.15	0.43	2.26	3.17(T ₂)	0.91	0.13	0.15
<i>m</i>-2CZP-BZ	2.28	2.96	0.34	2.18	3.06(T ₂)	0.88	0.28	0.41
<i>p</i>-2CZP-BZ	2.28	2.93	0.32	2.05	3.16(T ₂)	1.11	0.45	0.69
<i>o</i>-2POZ-BZ	2.28	2.27	0.01	1.86	2.69(T ₃)	0.83	0.41	20.5
<i>m</i>-2POZ-BZ	2.28	2.42	0.07	2.05	2.65(T ₃)	0.60	0.29	2.08
<i>p</i>-2POZ-BZ	2.28	2.21	0.03	2.00	2.49(T ₃)	0.49	0.24	3.46

Table S15. Calculated vertical excitation energies of singlet and triplet states, energy gaps, SOC constants (cm^{-1}), NAC constants (bohr^{-1}), k_{RISC} (s^{-1}) between S_1 and related T_n states, overlap integral β , k_p (s^{-1}) and k_f (s^{-1}) of the investigated molecules by BMK/6-31G (d, p) level (energy unit in eV).

Mol.	<i>o</i> -2CZP-BZ	<i>m</i> -2CZP-BZ	<i>p</i> -2CZP-BZ
E_{T_1}	2.26	2.18	2.05
E_{T_2}	3.17	3.06	3.16
E_{T_3}	3.27	3.30	3.26
E_{S_1}	3.20	3.23	3.00
E_{S_2}	3.38	3.42	3.34
$\Delta E_{T_2-T_1}$	0.91	0.88	1.11
NAC (T_2-T_1)	1.68	2.12	1.78
$\Delta E_{S_1-T_1}$	0.94	1.05	0.95
$\Delta E_{S_1-T_2}$	0.03	0.17	-0.16
SOC (T_1-S_1)	0.27	0.46	0.18
SOC (T_2-S_1)	0.43	0.56	0.34
$k_{\text{RISC}}(T_1-S_1)$	1.11×10^{-38}	2.10×10^{-48}	6.44×10^{-40}
$k_{\text{RISC}}(T_2-S_1)$	2.91×10^7	2.12×10^5	6.65×10^7
f_{em}	0.2438	0.3287	0.8057
ΔE_{em}	2.51	2.71	2.36
$\beta(S_1)$	0.5022	0.4472	0.5830
k_f	0.67×10^8	1.05×10^8	1.95×10^8
k_p	2.06×10^{-2}	3.11×10^{-2}	6.43×10^{-3}
Mol.	<i>o</i> -2POZ-BZ	<i>m</i> -2POZ-BZ	<i>p</i> -2POZ-BZ
E_{T_1}	1.86	2.05	2.00
E_{T_2}	2.13	2.14	2.05
E_{T_3}	2.69	2.65	2.49
E_{S_1}	2.07	2.07	2.01
E_{S_2}	2.32	2.40	2.06
$\Delta E_{T_2-T_1}$	0.27	0.09	0.05
NAC (T_2-T_1)	5.03	6.32	3.74
$\Delta E_{S_1-T_1}$	0.21	0.02	0.01
$\Delta E_{S_1-T_2}$	-0.06	-0.07	-0.04
SOC (T_1-S_1)	0.53	0.67	0.09
SOC (T_2-S_1)	0.47	1.14	0.21
$k_{\text{RISC}}(T_1-S_1)$	1.98×10^4	9.03×10^7	2.04×10^6
$k_{\text{RISC}}(T_2-S_1)$	1.54×10^8	9.72×10^8	2.54×10^7
f_{em}	0(0.0029) ^a	0(0.0031) ^a	0(0.0037) ^a
ΔE_{em}	1.22(1.24) ^a	1.33(1.34) ^a	1.35(1.36) ^a
$\beta(S_1)$	0.1191(0.1584) ^a	0.1199(0.1504) ^a	0.1145(0.1468) ^a
k_f	0(1.94×10^5) ^a	0(2.41×10^5) ^a	0(2.97×10^5) ^a
k_p	2.99×10^{-2}	7.05×10^{-2}	2.08×10^{-3}

^a: Data in parentheses are parameters from the molecular geometries with the specific dihedral angle $\alpha = 80^\circ$.

Figure S1. The TDM maps, the overlaps and distributions of electron-hole wavefunctions for the **BF**-based molecules.

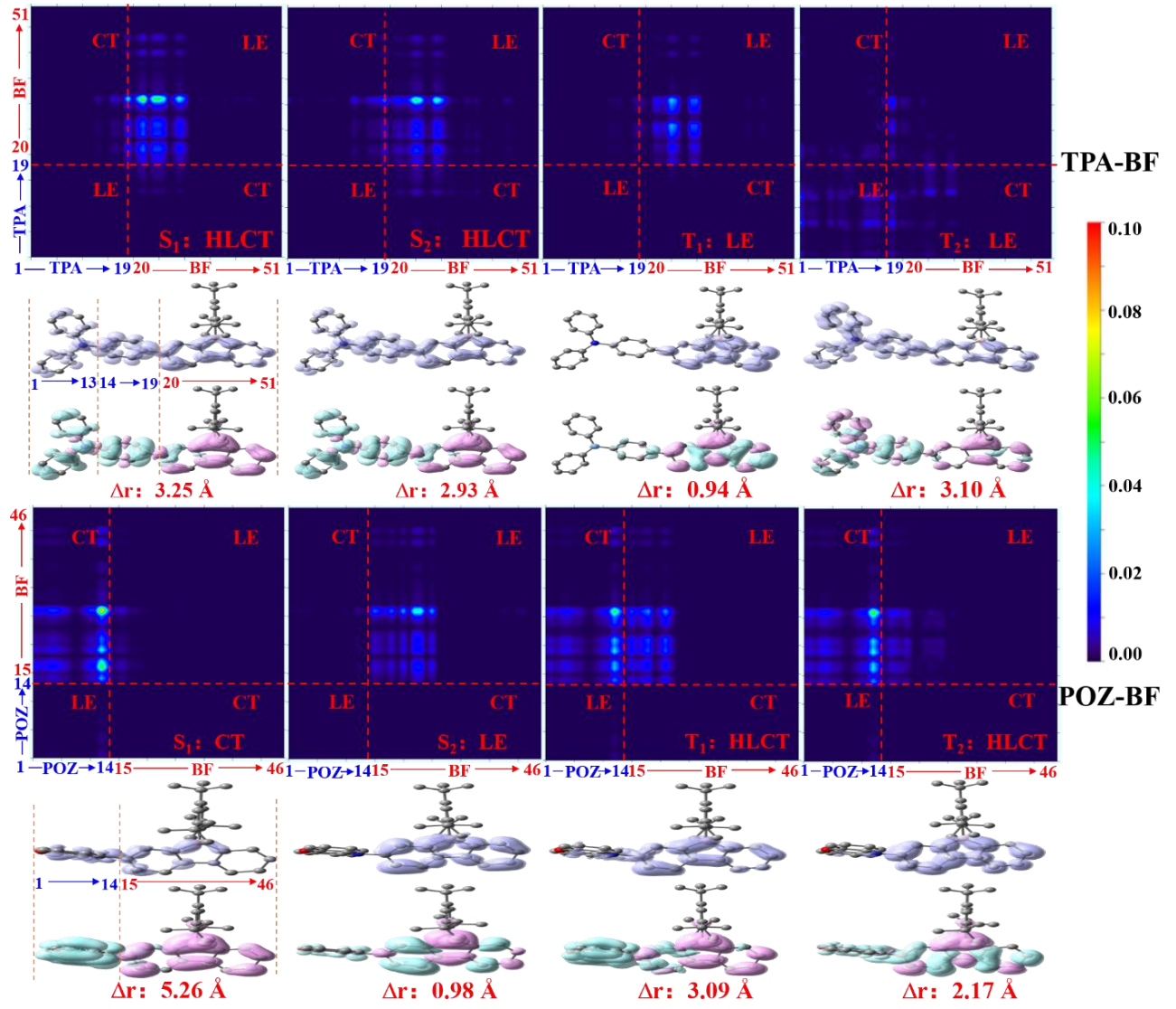


Figure S2. NTO analysis for the S_1 , S_2 , T_1 , and T_2 states and related energy diagrams of the state hybridization between LE and CT states for both singlet and triplet subspaces.

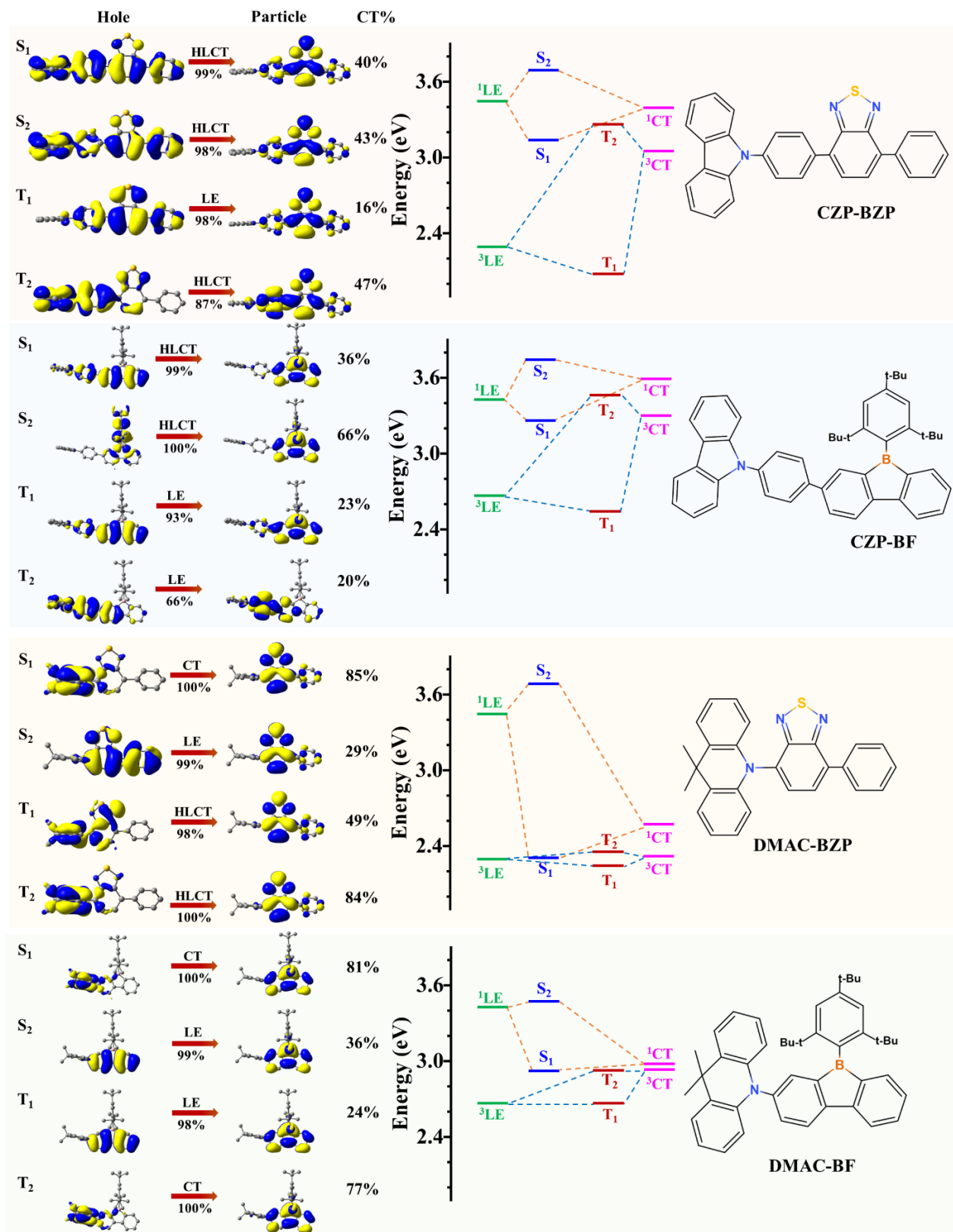


Figure S3. Calculated emission energies and oscillator strengths in S_1 states of the **POZ**-based molecules as function of the twisted angles. The blue dashed lines label the thermally activated energy at room temperature. The inserted structures are the optimized compounds with the lowest energies.

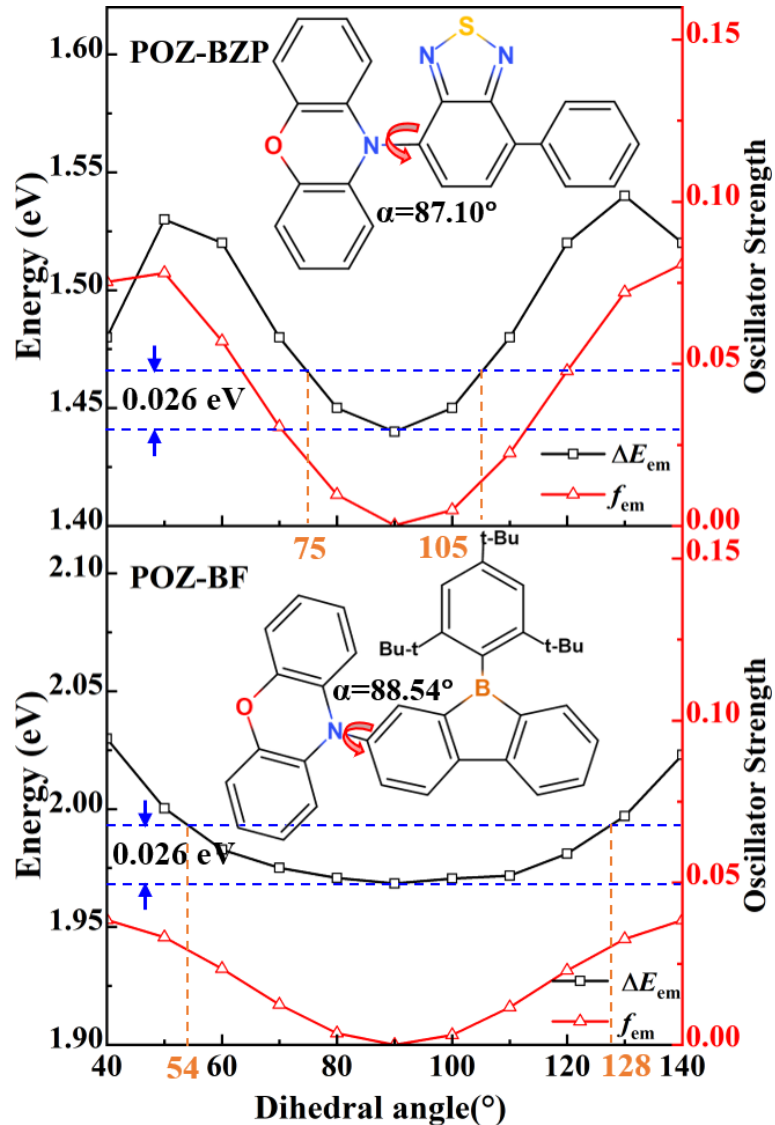


Figure S4. Chemical structures of the investigated D-A-D type molecules.

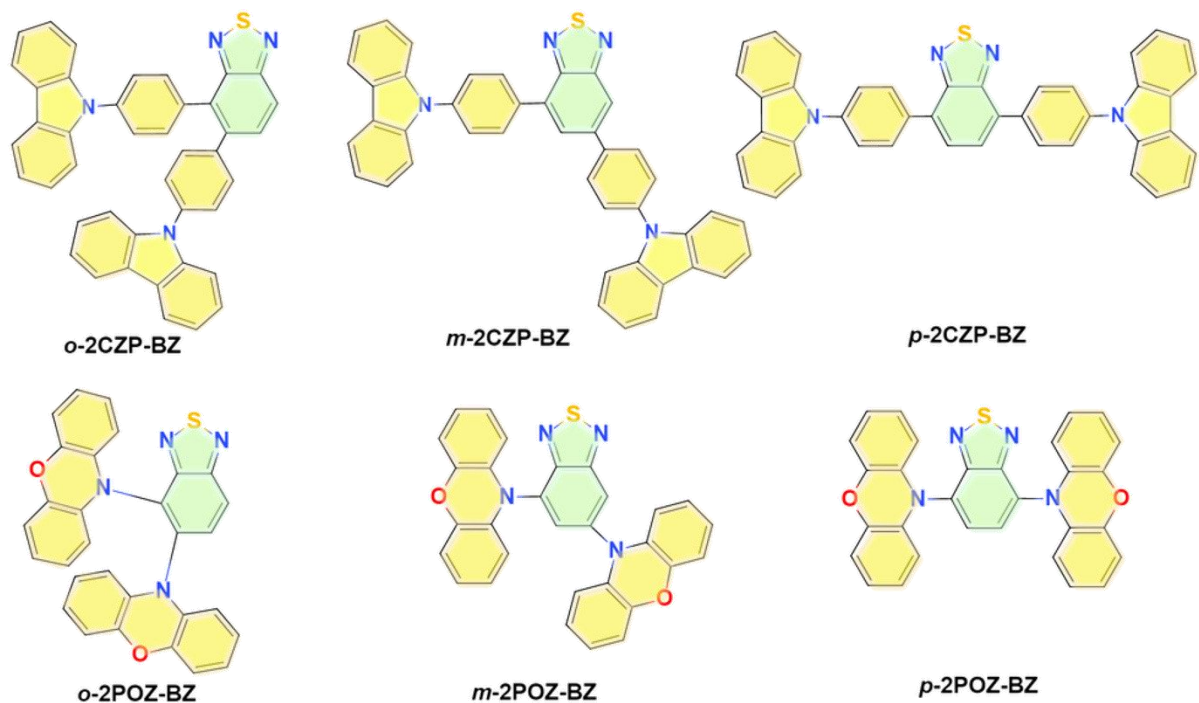


Figure S5. NTO analysis for the related excited states and energy diagrams of the state hybridization between LE and CT states of both singlet and triplet subspaces for D-A-D type HLCT molecules.

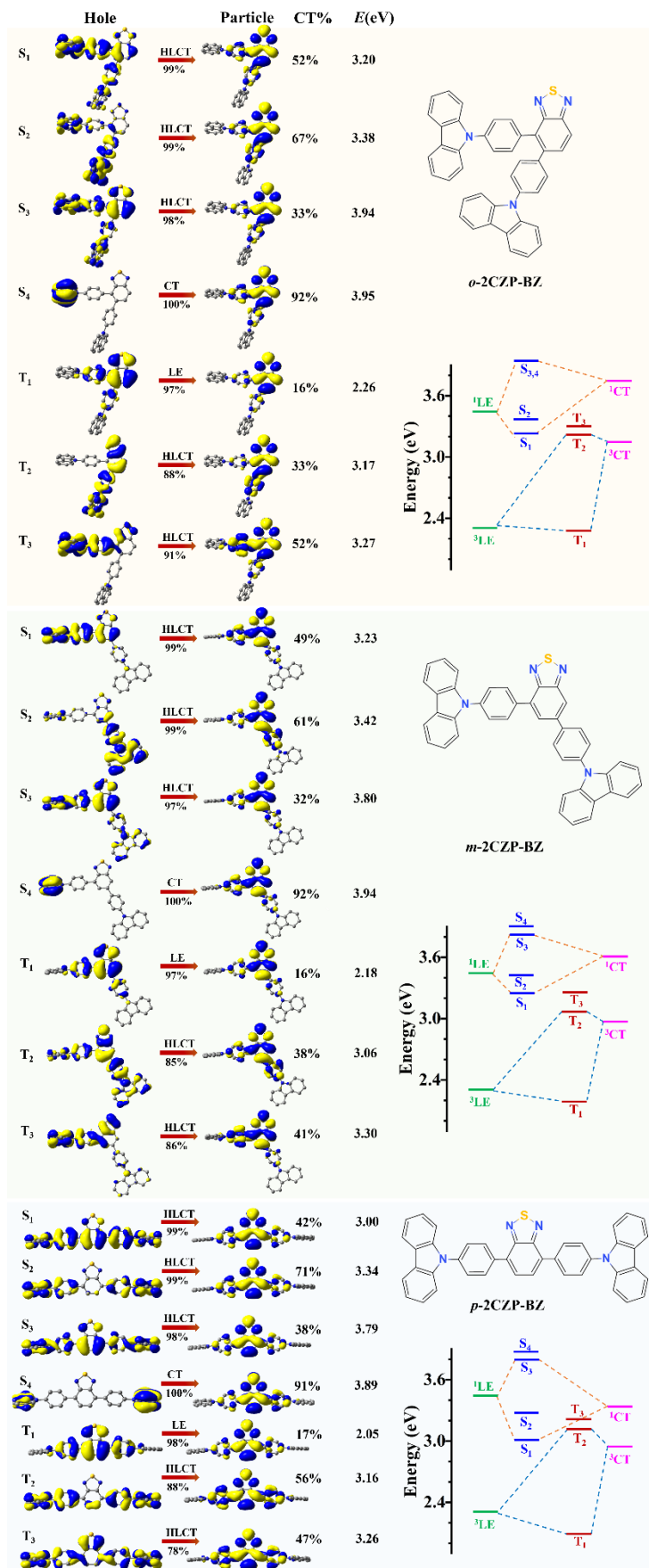


Figure S6. NTO analysis for the related excited states and energy diagrams of the state hybridization between LE and CT states of both singlet and triplet subspaces for D-A-D type TADF molecules.

